

## Is Fusion Inhibited for Weakly Bound Nuclei?

J. Takahashi, M. Munhoz, E. M. Szanto, N. Carlin, N. Added, A. A. P. Suaide, M. M. de Moura,  
R. Liguori Neto, and A. Szanto de Toledo

*Universidade de São Paulo, Instituto de Física, Departamento de Física Nuclear, Caixa Postal 66318, 05389-970 São Paulo,  
São Paulo, Brasil*

L. F. Canto

*Instituto de Física, Universidade Federal do Rio de Janeiro, Caixa Postal 68528, 21945-970 Rio de Janeiro, RJ, Brasil*  
(Received 2 August 1996)

Complete fusion of light radioactive nuclei is predicted to be hindered at near-barrier energies. This feature is investigated in the case of the least bound stable nuclei. Evaporation residues resulting from the  ${}^6\text{Li} + {}^9\text{Be}$  and  ${}^6\text{Li} + {}^{12}\text{C}$  fusion reactions have been measured in order to study common features in reactions involving light weakly bound nuclei. The experimental excitation functions revealed that the fusion cross section is significantly smaller than the total reaction cross section and also smaller than the fusion cross section expected from the available systematics. A clear correlation between the fusion probability and nucleon (cluster) separation energy has been established. The results suggest that the breakup process has a strong influence on the hindrance of the fusion cross section. [S0031-9007(96)02065-0]

PACS numbers: 25.70.Jj, 25.60.Gc, 25.70.Mn

Recent theoretical [1,2] and experimental [3,4] studies have investigated the role of neutron skins or halos in the fusion and reaction cross sections of neutron rich projectiles incident upon heavy targets. Usually, the coupling to excited states tends to lower the potential barriers, and the fusion cross section at near and sub-barrier energies is enhanced [2]. On the other hand, it has been claimed [1] that the large probability that such weakly bound projectiles dissociated along the collision leads to a reduction of the complete fusion cross section. Such investigations in the case of light systems are of fundamental importance in the context of astrophysics, where low energy radioactive nuclei interact strongly. In a previous work [5], we carried out a systematic study of the fusion cross section in light ion collisions. This study showed an inhibition of the yield as the system mass decreases, resulting from the progressive increase of the barrier height and the decrease of the barrier radius. This trend is observed [6] in collisions involving light nuclei where the binding energy per nucleon does not reach the saturation value  $B/A \sim 8$  MeV. Within this scenario, we performed a systematic study of fusion reactions involving the least bound stable nuclei in nature, as, e.g.,  ${}^6\text{Li}$  ( $S_\alpha = 1.47$  MeV),  ${}^7\text{Li}$  ( $S_\alpha = 2.45$  MeV), and  ${}^9\text{Be}$  ( $S_n = 1.67$  MeV). Although radioactive nuclei such as  ${}^{11}\text{Li}$  and  ${}^{11}\text{Be}$  with very low neutron separation energies [ $S_{2n}({}^{11}\text{Li}) \sim 0.3$  MeV] are not yet available with intensities which allow such kind of experiments, systematic studies with the proposed systems may shed some light on future studies with radioactive nuclei. In this paper we show that a clear correlation exists between the *fusion probability* ( $P_F$ ) and the separation energy ( $\varepsilon$ ) required for breaking up the colliding nuclei into fragments, and that the breakup process may account for most of the flux diverted from the fusion channel.

The experiments were performed using  ${}^6\text{Li}$  beams from the University of São Paulo Pelletron accelerator with energies ranging from 1 to 5 MeV/nucleon. Atomic  $\text{Li}^-$  and molecular  $\text{LiO}^-$  primary beams were extracted from a SNICS type ion source and used for the high and low energy data, respectively. Self-supporting C ( $\sim 80 \mu\text{g cm}^{-2}$  areal density) and Be ( $\sim 200 \mu\text{g cm}^{-2}$  areal density) targets were used. A very thin gold layer was deposited on the targets for normalization purposes. Carbon buildup was minimized during the exposure by surrounding the target with a liquid nitrogen cooled ring and by using a cryogenic pumping system.

Charged reaction products and evaporation residues were identified by means of a triple telescope consisting of an ionization chamber followed by a large area solid state detector (in order to identify the evaporation residues) and by a second and thicker solid state detector in order to detect the light ( $p$ ,  $d$ , and alpha) reaction products. Five of those telescopes were used simultaneously, separated by an angular interval of  $5^\circ$ . At very low bombarding energies, the energy threshold determined by energy losses at the window and gas became significant. At those energies, the detection system was complemented by a time of flight telescope (TOFT) consisting of a microchannel plate time detector used as a start detector and a large solid state silicon detector used to supply the energy and stop signals of the reaction products. Absolute values of the target thickness and detector solid angles were determined by fitting the elastic scattering angular distributions to optical model predictions [6]. Fusion-evaporation yields were measured at bombarding energies ranging from  $6 < E_{\text{lab}} < 33$  MeV, corresponding to the barrier energy and five times the barrier, respectively, and angular distributions were measured for the charge-identified reaction

products with  $6^\circ < \theta_{\text{lab}} < 55^\circ$ . The fusion-evaporation residues were distinguished from other reaction products by comparing their energy spectra to those expected for a statistically equilibrated compound nucleus, predicted by the Monte Carlo code LILITA [5,7]. Possible contribution of the incomplete fusion (ICF) process has been investigated within the same procedure. An upper limit for ICF yields has been estimated [see Figs. 1(a)–1(c)] and found negligible when compared to complete fusion (CF) yields ( $\frac{\sigma_{\text{ICF}}}{\sigma_{\text{CF}}} \leq 0.1$  up to  $E \leq 3V_B$ ). Unfolding procedure is shown in Figs. 1(a) and 1(b) for  $E_{\text{lab}} = 18$  MeV (energy for which the CF inhibition is expected to be maximum), as well as for the highest energy measured  $E_{\text{lab}} = 33$  MeV [Fig. 1(c)].

Excitation functions for the  ${}^6,{}^7\text{Li} + {}^{12}\text{C}$  and  ${}^6,{}^7\text{Li} + {}^9\text{Be}$  reactions are presented in Figs. 1(d)–1(g). Fits to the Glas and Mosel expression [8] were used to extract the values of the fusion barrier height ( $V_B$ ) and radius ( $R_B$ ) listed in Table I. The values for the barrier height appear to be larger than the ones obtained through an extrapolation from the systematics available in the literature for heavier systems [5]. This effect is also clearly observed when we compare the data to the predicted excitation functions based on the extrapolated ( $V_B^0, R_B^0$ ) values. A similar situation is observed with respect to the maximum value for the measured fusion cross sections ( $\sigma_{\text{max}}$ ), which appear to be much lower than the expected ones [9] (Table I).

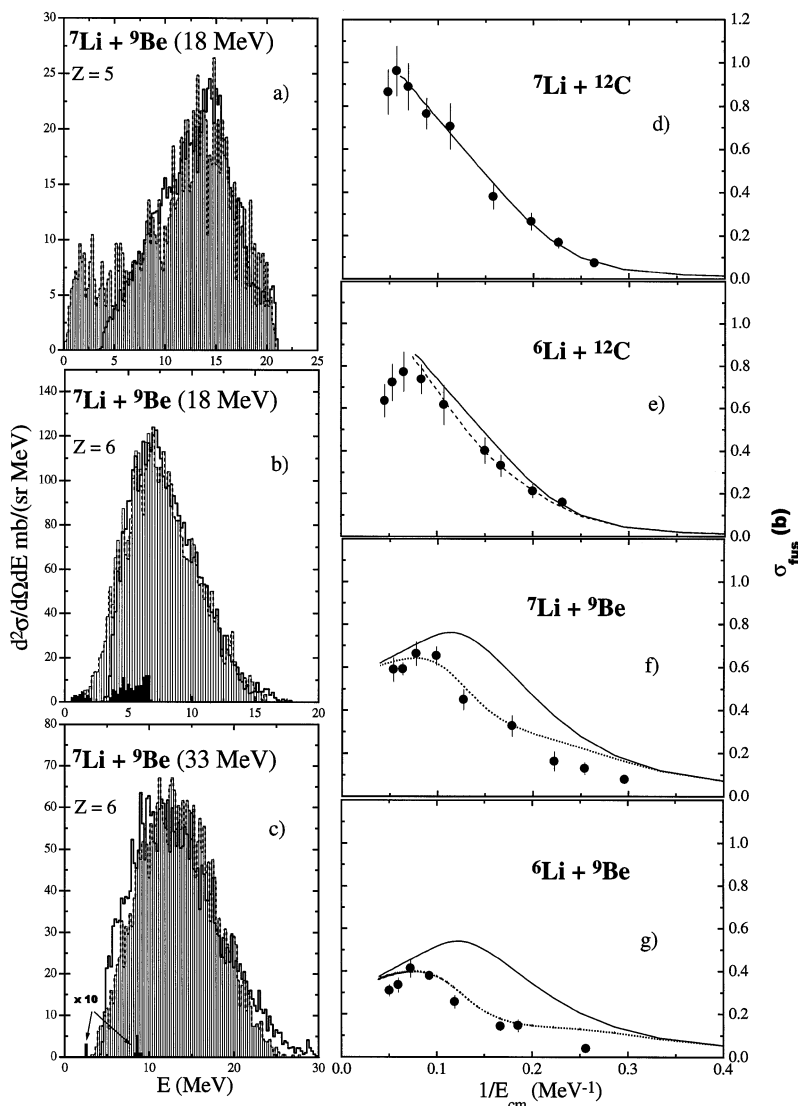


FIG. 1. (a)–(c), Energy spectra for  $Z = 5$  and  $Z = 6$  evaporation residues at  $E_{\text{lab}} = 18$  MeV (where a maximum fusion inhibition is expected) and  $E_{\text{lab}} = 33$  MeV (at the highest bombarding energy). The solid lines represent the experimental data. The dashed lines represent the statistical model prediction for complete fusion yields. The black spectra represent the predicted ICF contribution assuming an upper limit ( $\frac{\sigma_{\text{ICF}}}{\sigma_{\text{CF}}} = 0.1$ ), and the vertical bars represent the CF + ICF predicted spectrum assuming 10% of ICF. (d)–(g), Energy dependence of the fusion cross section for the  ${}^6,{}^7\text{Li} + {}^{12}\text{C}$  and  ${}^6,{}^7\text{Li} + {}^9\text{Be}$  reactions. Solid circles describe the experimental values. The solid curves represent the Glas and Mosel model calculations based on barrier parameters  $V_B$  and  $R_B$  extrapolated from the systematics of [5] and Table I. The dashed curves represent model prediction with no free parameters.

TABLE I. Values of various parameters discussed in text.

System	$V_B^a$ (MeV)	$R_B^b$ (fm)	$V_B^0^c$ (MeV)	$R_B^0^d$ (fm)	$\sigma_{\max}^e$ (mb)	$\sigma_{\max}^f$ (mb)
${}^7\text{Li} + {}^{12}\text{C}$	4.02	6.18	3.01	7.53	740	1020
${}^6\text{Li} + {}^{12}\text{C}$	4.63	6.31	3.03	7.52	730	900
${}^7\text{Li} + {}^9\text{Be}$	4.37	6.16	2.03	7.50	630	1106
${}^6\text{Li} + {}^9\text{Be}$	5.03	4.78	2.05	7.49	392	1250

<sup>a</sup>Value for the fusion barrier height ( $V_B$ ) obtained from fits of the experimental data to the Glas and Mosel expression [8].

<sup>b</sup>Value for the fusion barrier radius ( $R_B$ ) obtained from fits of the experimental data to the Glas and Mosel expression [8].

<sup>c</sup>Value for the fusion barrier height  $V_B^0$  obtained from the extrapolation of the systematic data presented in Ref. [5].

<sup>d</sup>Value for the fusion barrier radius  $R_B^0$  obtained from the extrapolation of the systematic data presented in Ref. [5].

<sup>e</sup>Experimental value ( $\sigma_{\max}$ ) obtained for the maximum fusion cross section.

<sup>f</sup>Expected value for the maximum fusion cross section ( $\sigma_{\max}^0$ ) from Ref. [9].

A fusion probability  $P_F = \sigma_F/\sigma_R$  can be evaluated by calculating, as a function of the bombarding energy, the ratio of the experimental fusion cross section  $\sigma_F$  to the reaction cross section  $\sigma_R$  estimated from the optical model fits to the elastic scattering data. An energy extended plateau can be observed for  $P_F$  at energies above  $E_{\text{cm}} \sim 2V_B$  (see Fig. 2) for all the systems investigated. At much higher energies ( $E_{\text{cm}} > 4V_B$ ) corresponding to regime II, where fusion is not a dominant process anymore, a decrease of  $P_F$  is expected. However, this en-

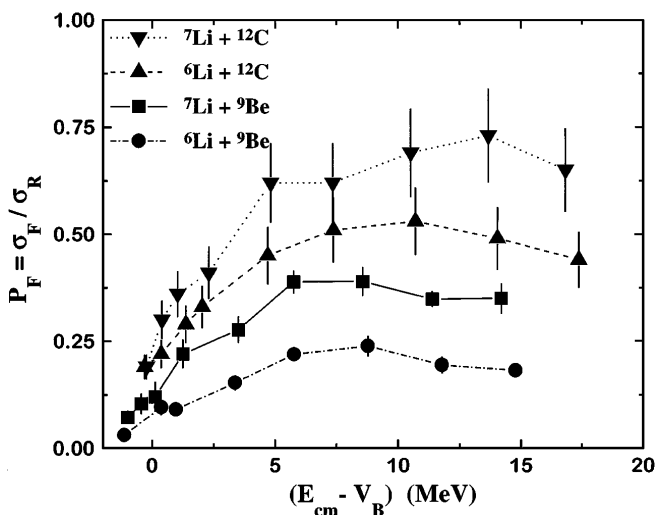


FIG. 2. Energy dependence of the fusion probability  $P_F = \sigma_F/\sigma_R$  for the  ${}^{6,7}\text{Li} + {}^{12}\text{C}$  and  ${}^{6,7}\text{Li} + {}^9\text{Be}$  reactions. The lines were drawn to guide the eye. The error bars reflect the experimental uncertainty in  $\sigma_F$ , as well as the uncertainty in the  $\sigma_R$  determination from the optical model calculation. The decrease of  $P_F$  at higher energies ( $E_{\text{cm}} \geq 4V_B$ ) due to the growing of important fast processes has not been investigated in the present work.

ergy domain is centered farther than the energy measured in the present work.

The dependence of the fusion probability on the effective breakup energy  $\varepsilon_e$  [13] which takes into account the separation energy of the target and projectile (presented in Fig. 3) indicates a clear correlation between the fusion probability and the separation energy of the colliding nuclei, especially for the weakly bound ones with  $\varepsilon < 2.5$  MeV (with values ranging from  $P_F \sim 0.8$  down to  $P_F \sim 0.2$  in the case of the  ${}^6\text{Li} + {}^9\text{Be}$  system).

To account for the effect of the separation energies ( $\varepsilon_e$ ) of the colliding nuclei on the fusion process, we employ the model of Ref. [1]. The effects of the breakup channel (b-up) on  $\sigma_F$  can be taken into account through the addition of the appropriate polarization potential to the optical potential in the entrance channel, in a single-channel calculation. Assuming that this polarization potential is dominated by its imaginary part, it will lead to a reduction of  $\sigma_F$ , and this reduction can be written in terms of a survival probability in each partial wave, expressing the fact that only the fraction of the incident flux that remains in the elastic channel contributes to fusion. The resulting inhibited fusion cross section can then be written as

$$\sigma_F = \frac{\pi}{k^2} \sum_{l=0}^{\infty} (2l+1) T_l^{\text{opt}} P_l^S,$$

where  $k$  is the wave number,  $T_l^{\text{opt}}$  is the transmission coefficient for the optical potential, and  $P_l^S$  is the survival probability [1]

$$P_l^S = 1 - T_l^{\text{b-up}} \\ = \exp\left[-\frac{4\mathcal{F}_0^2}{E_{\text{cm}}(E_{\text{cm}} - Q)} |S_l^{(1)}|^2 I_l^2(\eta, s, \xi)\right].$$

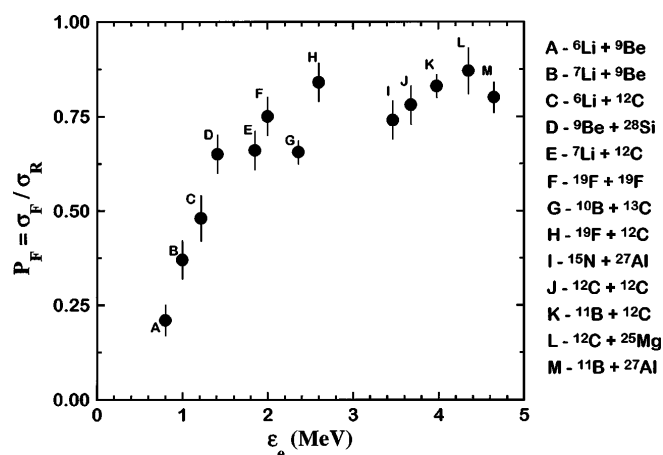


FIG. 3. Dependence of the fusion probability  $P_F = \sigma_F/\sigma_R$  on the effective separation energy ( $\varepsilon_e$ ) [13] for the  ${}^{6,7}\text{Li} + {}^{12}\text{C}$  and  ${}^{6,7}\text{Li} + {}^9\text{Be}$  reactions and other channels extracted from the literature [5,14]. Error bars are indicated and reflect the experimental uncertainty in  $\sigma_F$ , as well as the uncertainty in the  $\sigma_R$  determination from the optical model calculations. The points H, I, and J were extracted from Refs. [10,11,12], respectively.

Above,  $\mathcal{F}_0^2$  is the strength factor associated with the nuclear breakup process,  $Q$  is the  $Q$ -value for the breakup channel, and  $s_l^{(1)}$  is the partial-wave-projected elastic  $S$  matrix for a collision initiated in the breakup channel with energy  $E_{\text{cm}} - Q \cdot I_l(\eta, s, \xi)$  the integral of Coulomb wave functions (for details see Ref. [1])

$$I_l(\eta, s, \xi) = \int_0^\infty F_l(\eta_1, k_1 r) F_l(\eta_2, k_2 r) e^{-r/\alpha},$$

where  $\eta_1$  and  $k_1$  ( $\eta_2$  and  $k_2$ ) are, respectively, the Sommerfeld parameter and the wave number in the elastic (breakup) channel, and  $\xi = (k_1 - k_2)/(k_1 + k_2)$ . The parameter  $\alpha = \sqrt{2\mu_{bx}\varepsilon_s/\eta^2}$ , where  $\mu_{bx}$  is the reduced mass for the fragments  $b$  and  $x$  in the breaking nucleus and  $\varepsilon_s$  is the separation energy, measures the spatial extension of the relative wave function of the two fragments.

The generalization of this treatment for the breakup of both projectile and target is straightforward. In this case, one should use the survival probability

$$P_l^S = P_l^S(\text{projectile}) P_l^S(\text{target}).$$

For simplicity, we approximate all transmission factors by the Hill-Wheeler formula in our calculations. The model predictions for the excitation functions are presented in Fig. 1. No free parameters were used in these calculations. The coupling coefficient ( $\mathcal{F}_0^2$ ) has been scaled down to our systems, based on the expression extracted from Ref. [1]:

$$\mathcal{F}_0^2(A_p) = \mathcal{F}_0^2(^{12}\text{C}) \exp[2(R_p - R_T)/\alpha],$$

where  $\mathcal{F}_0^2(^{12}\text{C})$  is the coupling coefficient deduced in Ref. [1] for the  $^{11}\text{Li} + ^{12}\text{C}$  system,  $R_p$  ( $A_p$ ) represents the radius (atomic mass) of the projectile, and  $R^T$  represents the target radius. The experimental separation energies ( $\varepsilon_e$ ) of the  $^6,7\text{Li}$ ,  $^9\text{Be}$ , and  $^{12}\text{C}$  were used in the calculations. The ICF contribution has been estimated [15] within the same scenario. A two step process has been assumed in the sense that the breakup fragments [produced with a probability  $(1 - p_l^S)$ ] may fuse with the target with a cross section determined by a Hill-Wheeler transmission factor. This new fusion barrier is extracted from the systematics of Ref. [16]. A very satisfactory overall agreement has been achieved in most of the energy region investigated.

A study of the influence of the coupling coefficient and the breakup energy on the fusion cross section has pointed out [6] that the dominant factor in the hindrance of the fusion cross section is the effective breakup energy ( $\varepsilon_e$ ), and that its influence is concentrated at barrier energies. A decrease of the separation energy  $\varepsilon_e$  from 3 to 1 MeV reduces the fusion cross section an order of magnitude. A detailed investigation on the energy and angular momentum matching conditions of the reaction reveals that an angular momentum window is created,

being responsible for the localization of the effect around the barrier energies.

In summary, we have shown that the inhibition of the complete fusion channel in light weakly bound ion collisions is strongly correlated to the value of their binding energies. Model calculations support the interpretation that the breakup process may account for most of this feature. This result has important consequences within the scope of nuclear reactions of astrophysical interest, as well as in the newly growing field of interactions with light radioactive beams. Open questions still remain to be investigated as to the extent to which incomplete fusion contributes, as well as the identification of other peripheral competing processes.

This work was supported in part by the Conselho Nacional de Desenvolvimento Científico e Tecnológico (CNPq) and Fundação de Amparo à Pesquisa do Estado de São Paulo (FAPESP), Brasil.

- 
- [1] M. S. Hussein, M. P. Pato, L. F. Canto, and R. Donangelo, *Phys. Rev. C* **46**, 377 (1992).
  - [2] N. Takigawa, M. Kuratani, and H. Sagawa, *Phys. Rev. C* **47**, R2470 (1993); C.H. Dasso and A. Vitturi, *Phys. Rev. C* **50**, R12 (1994).
  - [3] A. Yoshida *et al.*, Proceedings of the 2nd RIKEN/INFN Joint Symposium, Riken, Saitama, Japan, 1995 (World Scientific, Singapore, to be published).
  - [4] C. Signorini *et al.*, Proceedings of the 2nd RIKEN/INFN Joint Symposium, Riken, Saitama, Japan, 1995 (World Scientific, Singapore, to be published).
  - [5] L. Fante, Jr., N. Added, R. M. Anjos, N. Carlin, M. M. Coimbra, M. C. S. Figueira, R. Matheus, E. M. Szanto, and A. Szanto de Toledo, *Nucl. Phys.* **A552**, 82 (1993).
  - [6] J. Takahashi *et al.* (to be published).
  - [7] J. Gomez del Campo and R. G. Stokstad, Report LILITA, ORNL, Report No. TM-7295 (unpublished).
  - [8] D. Glas and U. Mosel, *Nucl. Phys.* **A237**, 429 (1975).
  - [9] O. Civitarese, B. V. Carlson, M. S. Hussein, and A. Szanto de Toledo, *Phys. Lett.* **125B**, 22 (1983).
  - [10] B. Kohlmeyer, W. Pfeffer, and F. Puhlhofer, *Nucl. Phys.* **A292**, 288 (1977).
  - [11] F. W. Prosser Jr., R. A. Racca, K. Danshevar, D. F. Geesaman, W. Henning, D. G. Kovar, K. E. Rehm, and S. L. Tabor, *Phys. Rev. C* **21**, 1819 (1980).
  - [12] M. Conjeaud, S. Gary, H. Harar, and P. Wieleczko, *Nucl. Phys.* **A309**, 515 (1978).
  - [13] In order to account for the projectile and target separation energies, an effective value for the channel binding energy has been arbitrarily defined as  $1/\varepsilon_e = 1/\varepsilon_{\text{target}} + 1/\varepsilon_{\text{projectile}}$ .
  - [14] M. C. S. Figueira, E. M. Szanto, R. M. dos Anjos, N. Added, N. Carlin, L. Fante Jr., R. Matheus, and A. Szanto de Toledo, *Nucl. Phys.* **A561**, 453 (1993).
  - [15] P. Lotti *et al.* (to be published).
  - [16] L. Fante, Jr., N. Added, R. M. dos Anjos, N. Carlin, M. M. Coimbra, M. C. S. Figueira, R. Matheus, E. M. Szanto, and A. Szanto de Toledo, *Nucl. Phys.* **A552**, 82 (1993).